A low-cost spectrometer for NMR measurements in the earth's magnetic field[*]

Carl A. Michal[†]

Department of Physics & Astronomy, The University of British Columbia,
6224 Agricultural Rd, Vancouver, BC Canada V6T 1Z1
(Dated: Received 22 March 2010, in final form 8 July 2010 Published 9 August 2010)

We describe and demonstrate an inexpensive, easy-to-build, portable spectrometer for nuclear magnetic resonance measurements in the earth's magnetic field. The spectrometer is based upon a widely available inexpensive microcontroller, which acts as pulse-programmer, audio-frequency synthesizer, and digitizer, replacing what are typically the most expensive specialized components of the system. The microcontroller provides the capability to execute arbitrarily long and complicated sequences of phase-coherent, phase-modulated excitation pulses and acquire data sets of unlimited duration. Suitably packaged, the spectrometer is amenable to measurements in the research lab, in the field, or in the teaching lab. The choice of components was heavily weighted by cost and availability, but required no significant sacrifice in performance. Using an existing personal computer, the resulting design can be assembled for as little as US$200. The spectrometer performance is demonstrated with spin-echo and Carr-Purcell Meiboom-Gill pulse sequences on a water sample.

I. INTRODUCTION

Nuclear magnetic resonance (NMR) is a widely used technique for the study of materials of all kinds. Most modern NMR spectrometers are based on superconducting magnets, and operate with magnetic fields up to $\sim$ 20 T at frequencies up to 1 GHz. At the other end of the frequency regime however, earth's field NMR requires no superconducting magnet, but generally delivers much less information about the sample due to the loss of chemical shift resolution. Low frequency NMR however continues to be a subject of active research. Some current applications include studies of the liquid brine phase of sea ice in Antarctica [1–3] motivated by the importance of sea ice in global climate, the measurement of heteronuclear J-couplings[4, 5], the recent demonstrations that homonuclear J-couplings and chemical shifts can be observed at low field[6, 7], and the study of nuclear spin relaxation times in tissues, as at low fields T_1 times appear to be a promising way of identifying tumours[8]. Work on NMR in the earth's field has been recently reviewed[9].

Instrumentation for NMR at various magnetic field strengths, including earth's field, is available commercially, but commercial instruments are generally rather expensive due to the use of highly specialized components. Most commercial NMR systems incorporate a proprietary pulse programmer and discrete frequency synthesizers. In this work we describe a simple earth's field NMR spectrometer, in which the expensive specialized components are replaced with inexpensive, easy-to-find, general-purpose, mass-market components. While the system constructed here is intended for use in a teaching lab, it could be easily adapted for use in the research lab, or in the field. Two of the most important aspects of this device are its low cost ($\sim$ US$200, plus a notebook computer) and simplicity. Despite the extraordinarily low cost, few sacrifices, and in fact some gains, are made in the performance and flexibility of the device compared to similar research apparatus previously reported. This implementation makes NMR spectroscopy available to any researcher or student.

II. DESCRIPTION

A simple pulsed-NMR experiment begins with the application of a near-resonant excitation pulse applied to a coil containing the sample of interest. This pulse tips the nuclear magnetization from its equilibrium orientation, along a static magnetic field, into the plane perpendicular to the field. Following the pulse, precession of the magnetization about the static field induces a voltage in a receive coil. This signal is amplified, filtered, and digitized for further processing and display. One attractive feature of NMR in the earth's field is that if care is taken in siting and choice of materials, the field over the sample volume can be very uniform, giving NMR linewidths significantly less than 1 Hz. Because the net nuclear magnetization in thermal equilibrium at room temperature in low field is very small, such NMR experiments are often preceded by a polarization period, during which a much larger, but potentially more inhomogeneous, magnetic field is applied in order to increase the net polarization of the nuclear spins.

More sophisticated NMR experiments may involve applying more pulses, and demand that the phase and/or amplitude of the pulses be modulated. Signal averaging, which is often required to increase the signal-to-noise of

---

[†] michal@physics.ubc.ca

the received signals, requires a stable frequency source and reproducible pulse and analog-to-digital converter (ADC) timings.

The device to be described is a simple but versatile NMR spectrometer capable of executing arbitrarily long and complex pulse sequences reproducibly with sub-microsecond timing resolution. It can produce trains of phase-coherent audio-frequency pulses that can be phase modulated, and can digitize signals with 10-bit resolution at nearly 10 kHz for arbitrarily long periods.

The design of the current device draws deeply on that of Callaghan, Eccles and Seymour[10], but simplifies some aspects of their design, and replaces the most expensive, specialized, components with inexpensive, flexible, and widely available ones. Most significantly, Callaghan *et al.* used a specialized NMR console as a pulse programmer, audio frequency synthesizer, and digitizer. Here, we replace this expensive component with a small, easily acquired $30 microcontroller board. Other components of the current design are also optimized for ease of acquisition and cost. The current device can easily be built by anyone competent with a soldering iron.

A block diagram of the spectrometer is shown in figure 1. The present design uses two coils, one transmit/receive coil used to apply audio-frequency pulses and detect the NMR signals, and a second, larger coil for polarizing the nuclear spins. Details of the coils are collected in table I. The transmit/receive coil is perhaps the most challenging component of the spectrometer to construct, as it consists of 10 layers and some 3100 turns of AWG 30 copper wire (McMaster-Carr, Los Angeles, CA), wound on a section of 3" ABS drain-waste-vent (DWV) pipe, acquired from a local building supply store. This coil was wound on a Meteor ME 301 coil winding machine (Meteor AG, Wollerau, Switzerland). The sample is placed in an 0.5 ℓ polycarbonate bottle (Nalgene, Rochester, NY) which fits snugly inside the ABS form.

The polarization coil consists of three layers of AWG 18 copper wire, wound by hand on a section of 4" ABS DWV pipe. The windings of the polarization coil are connected in parallel to allow the use of a 5 V power supply that had been removed from an old personal computer. In operation, the coil draws 13.4 A and produces a field of approximately 10.5 mT, about 200 times the earth's field. The current to this coil is switched by means of a pair of high-current MOSFETs (IRFP4768, International Rectifier, El Segundo, CA). The nuclear magnetization, which develops along the coil axis during polarization, is adiabatically rotated to point along the earth's field by turning off the current over $\sim$ 10 ms. Another alternative would be to turn off the polarization current suddenly, leaving the magnetization pointing perpendicular to the earth's field. A rapid enough turn-off of the polarization coil is easily achieved (by charging a high-voltage capacitor through a diode when the MOSFETs turn off) if the polarization coil is isolated, however, with the much higher inductance of the detection coil strongly coupled

TABLE I. Coil Details

	T/R coil	Polarization Coil
diameter (cm)	10	15
length (cm)	10	15
wire size (AWG)	30	18
layers	10	3 (in parallel)
turns per layer	310	125
inductance	700 mH	900 μH
resistance (Ω)	310	0.34

to the polarization coil, producing such a rapid turn-off is problematic, as the detection coil is self-resonant at about 5 kHz. A schematic of the circuit used to drive and shut-off the polarization coil is shown in figure 2a. After the MOSFETs turn off, the current in the coil is turned off exponentially with a time constant of RC. This resistor/capacitor combination, with the polarization coil inductance, forms an over-damped series RLC circuit.

Use of an opto-isolator to drive the MOSFETs allows one side of the coil to be grounded at all times, and the 9V supply used to power the MOSFETs is simply a 9V alkaline battery. The relay allows the coil to be shorted, which, as suggested by Callaghan *et al.* [10], helps to shield the detection coil from audio frequency pick-up. The 5 Ω, 10 W resistor is required by the power supply. Most personal computer power supplies have maximum and minimum loads beyond which they shut down. This 5 Ω resistor draws 1 A, enough to keep the supply used here in its operating range when the coil is not drawing current.

A diagram of the audio-frequency transmitter is shown in figure 2b. Two logic lines from the microcontroller board are used to generate positive and negative lobes of the transmitter waveform to allow accurate phase cycling of the audio frequency signal. These two signals are combined by an op-amp subtraction circuit, passed through a low-pass Bessel filter, and amplified or attenuated to the level desired. Waveforms from before and after the filter, acquired with a Tektronix 3052 digital oscilloscope, are shown in figure 3. The duty cycle of the digital drive is restricted in order to reduce the harmonic content of the sum signal.

The receiver, figure 2c, consists of three low-noise op-amps (LT1007, Linear Technology, Milpitas, CA), one of which is configured as a band-pass filter. The final op-amp adds a 2.5 V dc offset to shift to the middle of the 0-5 V ADC voltage range. The LT1007 was chosen for its noise performance, low-cost, and the fact it uses the same pin configuration as many standard op-amps (eg. 741, and 411). This last aspect is expected to be important in a teaching lab, where a common pin-out should help to prevent op-amp mis-wiring. The overall gain of the receiver is about 50000. The receive coil is tuned to resonance with a fixed 18 nF capacitor located at the receiver.
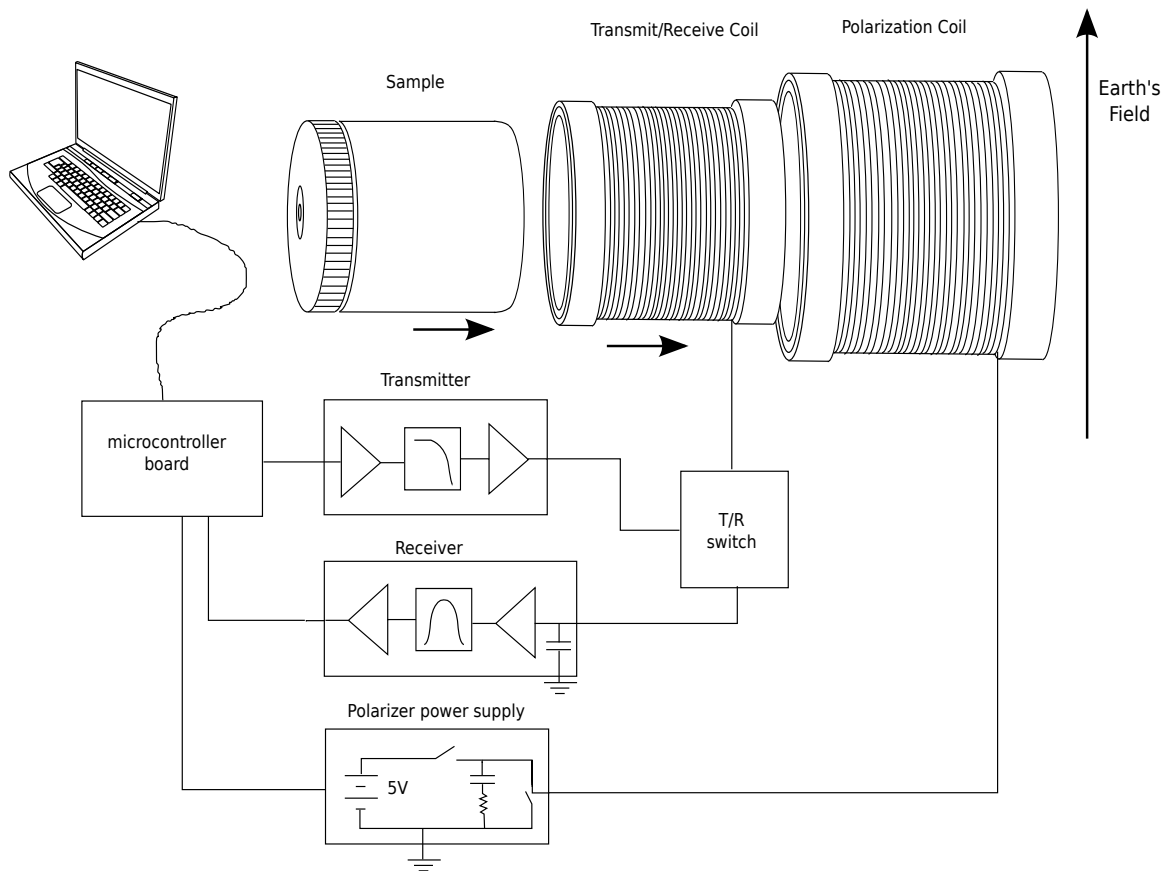
FIG. 1. Block diagram of the earth's field NMR spectrometer

The transmit/receive switch consists of three small reed relays, whose drive requirements (40 mA) are satisfied by the digital outputs of the microcontroller. The digital outputs driving the relays are protected from voltage spikes on relay shut-off by small signal diodes (1N4148, not shown) connected across each relay coil. Upon switching between transmit and receive, a receiver dead-time of 10 ms is found between the end of the pulse and the beginning of signal acquisition. The order of magnitude of this time is in agreement with that expected, as a resonant circuit having a Q of 5.8 (see appendix) at a frequency of 2 kHz would have a decay time constant of 2.8 ms. Thus any switching transients can be expected to decay on this time scale.

The microcontroller board, which acts here as pulse-programmer, audio-frequency synthesizer, and digitizer, is an Arduino Duemilanove, based on the ATmega328 microcontroller (Atmel, San Jose, CA). Arduino is an open-source hardware and software platform that greatly simplifies the use of the ATmega. Arduino boards are available from numerous vendors, and a complete integrated development environment is freely available[11]. Arduino boards incorporate a USB to serial converter chip, allowing a single USB connection to the host computer, through which programs are burned into the microcontroller flash, communications with the board are established when operating, and power to the board may be supplied. With the 16 MHz crystal oscillator on the Duemilanove, the ADC achieves its maximal 10-bit resolution at a maximum sample rate of 9615 samples/sec, more than adequate for capturing the $\sim$ 2 kHz signals in the earth's field. Because the ADC sampling frequency is more than twice the signal frequency and the signals all appear within a bandwidth much smaller than the ADC sample rate, no quadrature detection is necessary. All of the information that would be available from a quadrature receiver is retained by the single channel ADC.

The microcontroller board, if programmed carefully, is capable of producing trains of phase coherent pulses with reproducible timing, allowing not only accurate signal averaging, but phase cycling as well. The frequency stability of the system is determined by the stability of the oscillator driving the microcontroller. Here, the oscillator is an inexpensive crystal oscillator, Citizen HC49US (supplied with the Arduino board). This oscillator has a specified stability of $\pm$ 50 ppm over the temperature range of -10 to 60°C, corresponding to a variation in measured resonance frequency of about 0.2 Hz over this 70° temperature range. Because the frequency of such crystal oscillators depends on temperature in a deterministic way, the stability will be much better than this for more modest temperature variations. For field-work un-
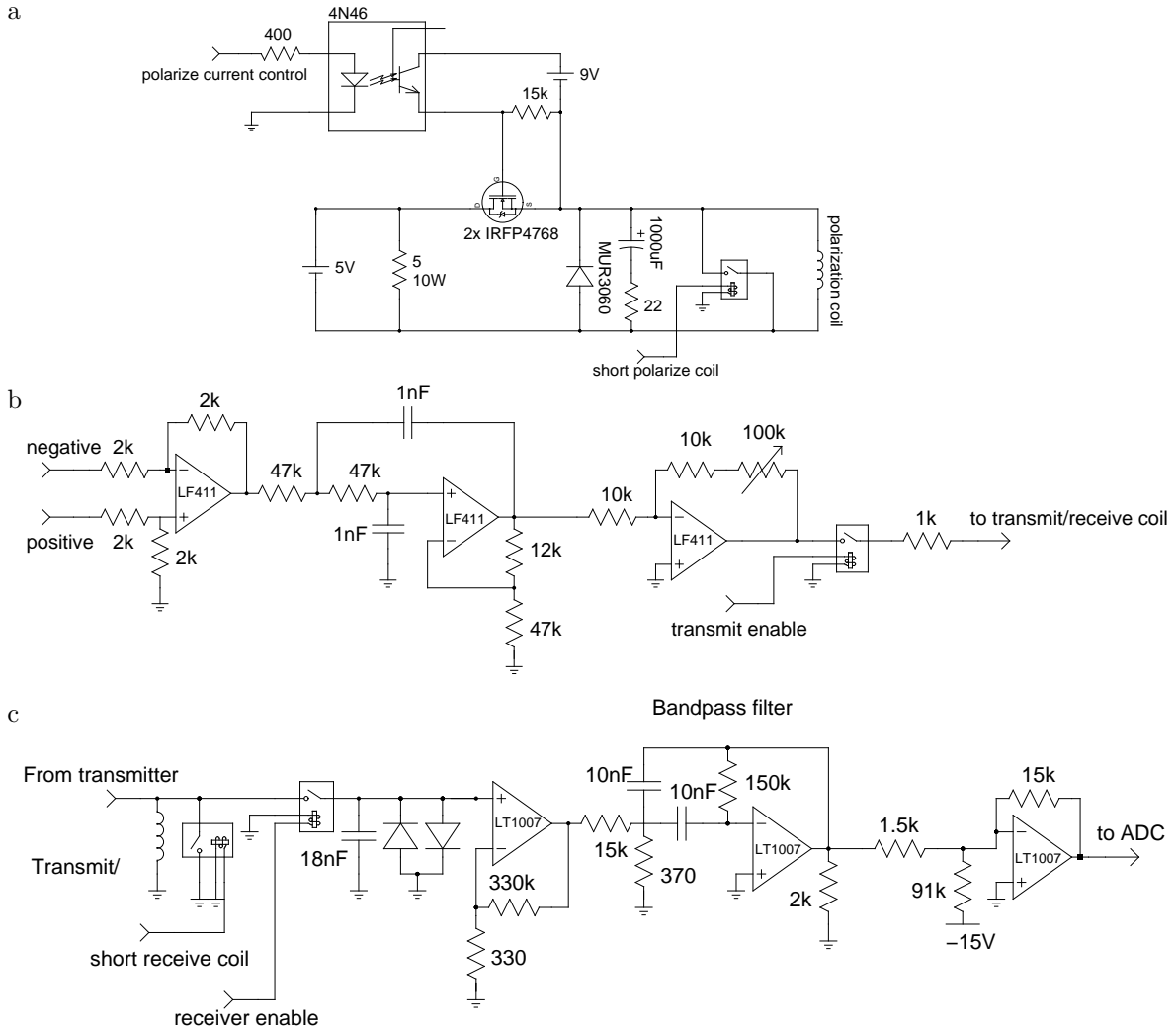
FIG. 2. Schematic diagrams showing the circuits used for a) the polarizing coil driver, b) the audio frequency transmitter, c) the receiver. All relays are Hamlin HE3351A055.

der extreme conditions, a temperature controlled oscillator could be employed.

For the experiments demonstrating the device below, the pulse-programming logic is performed in real-time on the microcontroller. While the programs written to date have used only a very small fraction of the available memory of the microcontroller, it is conceivable that a complicated pulse program would either not fit in the microcontroller's available memory, or would be too computationally intensive to run in real-time. Either situation however could be avoided by employing the microcontroller essentially as a state machine, and downloading pre-calculated states and durations from the host computer. This would allow arbitrarily long and complex pulse sequences to be executed. Data from the microcontroller's ADC is uploaded "on-the-fly" to the host computer allowing as many data points to be acquired as desired.

Programs that execute on the Arduino are writ-

ten in C/C++, and a simple C program was written to execute on the host computer to trigger sequence start and receive the acquired data. Both the microcontroller code and the program used to communicate with it have been made available at: http://www.phas.ubc.ca/~michal/Earthsfield.

A list of all of the major components in the spectrometer is presented in table II. This list sums to $187, and does not include resistors, capacitors, small-signal diodes, hook-up wire, or breadboards on which to build the circuits. In addition, a computer is required to program the microcontroller and accept the digital data. The Arduino software is multiplatform, available for Windows, Mac OS X, and Linux. The computer required here must run a supported operating system and have an available USB port.

The problem of audio-frequency pick-up is ubiquitous in low-frequency NMR, and has generally been handled either by extensive shielding or the use of two opposing
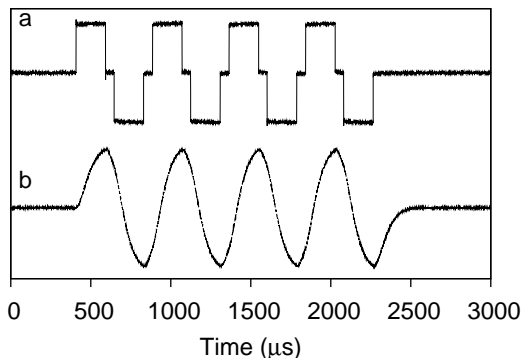
FIG. 3. Transmitter waveforms. a) shows the output from the summing amplifier, while b) shows the result following the low-pass filter.

TABLE II. Major Components

Component	Cost	Source
Arduino Duemilanove	$30	Sparkfun Electronics
aluminum shielding	$42	Metal Supermarkets
18 # copper wire	$28	McMaster-Carr
30 # copper wire	$23	McMaster-Carr
LT1007 op-amps	$3 \times 3	Digikey Corp.
LF411 op-amps	$3 \times 2	Newark Electronics
HE3351A055 relays	$4 \times 3	Newark Electronics
IRF4768 mosfet	$2 \times 9	Newark Electronics
MUR3060 diode	$5	Digikey Corp.
4N46 optoisolator	$4	Digikey Corp.
ABS pipe and fittings	$10	local building supply store
PC power supply	$0 - $15	used (or e.g. newegg.com)

coils, so that the pick up of environmental noise from the two coils cancels[9]. We found that the shielding provided by shorting the polarization coil to be insufficient in most locations tested, as harmonics of the power line dominated the acquired signals. Additional shielding was provided inexpensively by a placing the coil assembly inside a 30 cm length of 15 cm diameter, 7 mm wall aluminum tubing (Metal Supermarkets, Vaughan, ON). A thick shield is required as the skin-depth at these frequencies is substantial, approximately 2 mm in aluminum at 2 kHz. With this shielding in place, the NMR signal dominates the spectrum, as can be seen in figure 4b. Adding end caps to the shield tube made little further improvement.

Before the shielding was installed, an attempt was made to eliminate the power-line pick up by synchronizing the acquisitions with the power line. A low-voltage AC transformer powered from the mains was connected to one of the Arduino's digital inputs, and the pulse sequence triggered from the power line. With the phase-cycling used, pick-up from the power line is then sub-tracted on alternate transients. While this technique was found to work very well for short times, phase variations in the power line on time scales of ~ 0.5 s prevented effective cancellation for long-lasting signals.

III. RESULTS AND DISCUSSION

NMR signals acquired with the device described above, from an $0.55 \ \ell$ sample of tap water are shown in figure 4. The free-induction decay in figure 4a is the result of averaging four transients of a spin-echo pulse sequence, with a 10 ms echo time. The spectrum corresponding to this time-domain data is shown in figure 4b. The data was zero filled from 16384 to 32768 points, Fourier transformed, and phase adjusted, but not otherwise manipulated. A nutation plot is shown in figure 4c. The phase adjustment applied to all spectra in figures 4b and c was identical. The small variation in phase between the various spectra in the nutation plot is due to a small (~ 10 Hz) frequency offset from resonance of the transmitter. In each case, a simple phase cycle in which the phase of the first pulse was alternated between zero and π, and signals alternately added and subtracted was used. The phase of the inversion pulse was fixed.

The multiple pulse capability of the system is demonstrated in figure 4d, where the field homogeneity was purposefully degraded slightly and a Carr-Purcell Meiboom-Gill sequence[12] was used to create a train of 16 echoes. Signal intensity remains visible 7 s after the initial 90° pulse.

The enhancement of the signal achieved by polarizing in the polarization coil was measured by comparing the signals observed with the polarizing coil active to those without. These data are shown in figure 5. Integrals of the NMR peaks in these data indicate an enhancement of approximately 182, compared to the 212 fold increase in polarization field, indicating that relatively little magnetization is lost in the adiabatic field turn-off. This also demonstrates the stability of the device, as the spectrum acquired without the polarization coil averaged over 14 hours.

Callaghan *et al.* have discussed the calculation of the signal to noise ratio expected from their device in detail[10], and the calculation for the present device is similar. The details are discussed in Appendix A. The magnitude of the signal observed is in excellent agreement with that expected, while the noise measured in an indoor urban environment is some 2.2 times larger than calculated. We find a typical time-domain signal to noise ratio (SNR) of 24 for a single shot experiment in an indoor, urban environment, with much of this noise arising from isolated power-line harmonics. The most important differences between Callaghan's device and the present in terms of sensitivity is that the polarization field used here is about a factor of three less strong, and additional shielding is used here. As can be seen by comparing figure 4a to Callaghan's figure 7b, which shows the average
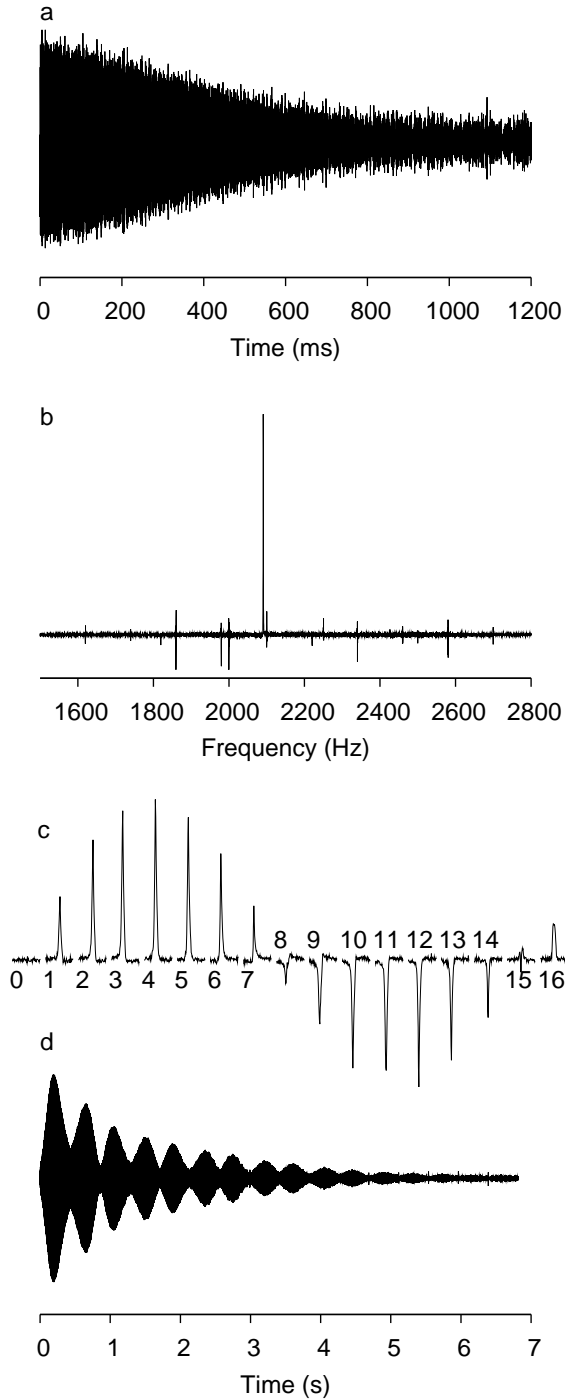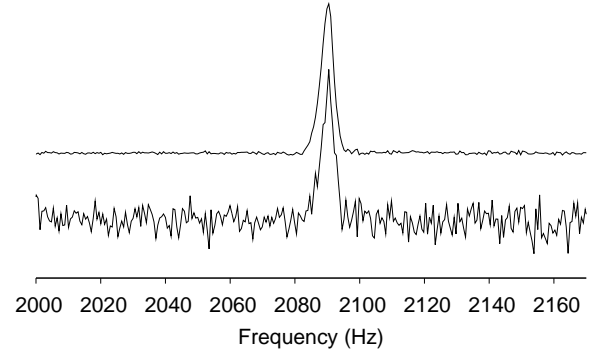
FIG. 5. Polarization enhancement from the polarization coil. The lower trace is the result of 7500 transients with a 7 s recycle delay. The upper trace is the result of 44 transients with the polarization current on for 7 s. The vertical and horizontal scales of both data sets are identical, but the traces are offset vertically for clarity.

FIG. 4. NMR signals. a) shows the decay following a spin-echo pulse sequence. b) is the spectrum corresponding to a), while c) shows the variation in signal observed as the duration of the initial pulse is varied. The numerical labels indicate the number of full audio-frequency cycles applied. d) shows the result of a Carr-Purcell Meiboom-Gill multi-echo sequence with 16 echoes. a) and b) are the result of four transients, each spectrum in c) was acquired with two transients, while d) was 256 transients. Most of the noise spikes in b) correspond to odd harmonics of the 60 Hz power-line frequency.

of four times as many transients with a polarization field three times larger, the present device compares very well. Despite the six-fold disadvantage from the reduced polarization field and smaller number of transients, the SNR here appears to be similar or better. This difference however, is entirely due to the increased shielding provided by the aluminum tubing. In both cases the receiver contributes negligibly to the noise.

The SNR observed in the frequency domain depends sensitively on the homogeneity of the magnetic field over the sample volume. The homogeneity shows an extreme dependence on the location of various objects nearby, and in fact can be improved by "shimming" with objects at hand. The linewidth (full-width at half-maximum) in figure 5 is about 5 Hz, but in figure 4, an aerosol spray can (of compressed air) was moved to about 30 cm distant from the coil assembly, yielding a linewidth of ~ 0.6 Hz. In the outdoors, significantly narrower linewidths are more easily achieved. In figure 6, a spectrum that was acquired at a local beach is shown. This spectrum was acquired with thermal polarization in the earth's field, *i.e.* with no current in the polarization coil, and is the average of 64 transients, acquired over about 10 minutes. The full-width at half-maximum of the line is about 0.21 Hz, not much greater than the best possible linewidth of 0.18 Hz, based on the measured T_2 of 1.75 s.

Spectra and T_1 relaxation measurements have also been collected of an apple (145 g), a banana (128 g), and an intact aluminum can containing 355 ml of beer. The T_1 measurements were accomplished by adding a variable delay following the polarization period before apply the audio-frequency pulse and fitting the resulting magnetization decays to decaying exponentials. With substantial variation in signal intensity and minor variations in lineshape, attributable to the different geometries of
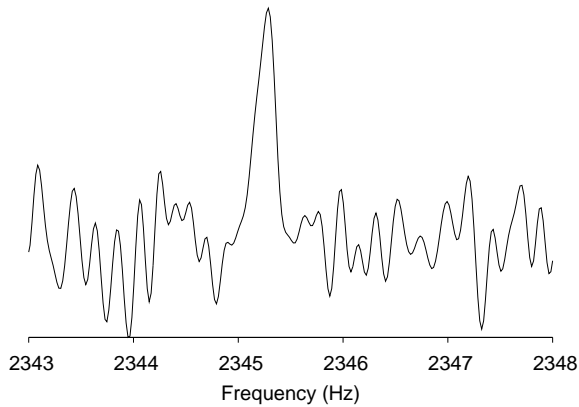
FIG. 6. Earth's field NMR spectrum of thermally polarized water.

the samples, the spectra are essentially indistinguishable from that of the water sample. In contrast to the spectra, the T_1 times of these samples vary significantly. For the tap water sample $T_1 = 2.3 \pm 0.1$ s, while for the beer it is notably shorter, 1.5 ± 0.15 s. For the apple, $T_1 = 1.0 \pm 0.1$ s, and the banana has $T_1 = 690 \pm 55$ ms. While the choice of these samples may appear whimsical, a great deal of research has been undertaken in food science with NMR (see [13] for example), and many more research opportunities exist in this area. A widely available low-cost spectrometer may accelerate such work. The fact that NMR measurements are possible on a liquid in an enclosed aluminum container is a testament to the ability of these low frequency electromagnetic signals to penetrate conductors that would completely shield the radio frequencies used in high-field NMR.

The device used to collect all of the data shown above was built in a form most suitable for a teaching lab, as that is its intended use. The transmitter and receiver were constructed on a single 5 x 16 cm breadboard, while the polarization coil driver, due to the high current handling required of its components, was soldered together on a prototyping board. With a little effort at packaging the device in a robust manner, it could easily be configured for regular use in the field. It is small enough to be transportable in a single trip by bicycle. The transmitter/receiver combination draws a total of 16 mA from its supplies, making it suitable for battery powered operation, two 9V batteries would suffice for $\sim$ 20 hours. The Arduino board is powered by its USB connection to a notebook computer. The computer power supply for polarizing the nuclei however requires on the order of 100 W. This requirement is easily met with a modest lead acid battery and inverter. Alternatively, the polarization coil could be powered directly from such a battery, either with the coil connections in parallel for a 6V battery, or in series for a 12 V battery. A 6 V 12 A-hr sealed lead acid battery has a mass of < 2 kg (e.g. Panasonic LC-R0612P, available from Digi-key), and two of these in parallel could power the polarization coil at 50% duty cycle for more than two hours.

As described, the present device is capable of producing any desired sequence of phase-coherent audio-frequency pulses, and so can be used for performing a wide variety of pulsed NMR experiments, including one-dimensional spectroscopy, relaxation measurements such as inversion recovery, spin-echo, and Carr-Purcell-Meiboom-Gill sequences, as well as two-dimensional heteronuclear (e.g. ^{19}F-^{1}H) NMR experiments. Potential field applications include measuring moisture content and nuclear-spin relaxation parameters,(of, for example, soil, fruit, ice, etc.) and geomagnetic studies of the spatial and/or temporal variation of the earth's field. In the teaching lab, the device could be provided fully assembled for use in exploring NMR and spin physics, or could be presented only partially complete, where students would build some significant fraction of the circuitry and the focus would be more on instrument building. At present the device has no pulsed-field gradient capability. Adding one field gradient for diffusion measurements or multiple gradients for imaging would be relatively straightforward. The Arduino has a number of additional digital outputs to facilitate control of these devices.

IV. CONCLUSIONS

In conclusion, we have presented a low-cost, easy-to-build earth's field NMR spectrometer suitable for use in research and teaching environments. The only specialized piece of equipment used in the construction was a coil-winding machine that was used to wind the 3100 turn detection coil, although a resourceful builder without access to such a machine could surely wind an acceptable coil by hand or with an improvised coil winder. A key component of this device is an inexpensive, easy-to-program microcontroller board that acts as high-performance pulse-programmer, audio frequency synthesizer, and analog-to-digital converter. The low cost, accessibility of components, and simplicity makes such a device available to any researcher or student.

Appendix A: Signal and Noise calculations

Ideally, the noise in an inductively detected NMR experiment is dominated by Johnson thermal noise from the coil resistance, and is given by[1]

$$V_{\text{Johnson}} = \sqrt{4 k_B T \Delta f R} \qquad (A1)$$

in which k_B is Boltzmann's constant, T is the temperature of the coil, Δf is the noise bandwidth, and R is the coil resistance.

The signal expected can be expressed as

$$V_{\text{signal}} = \left(\frac{B_1}{i_1} \right) V \omega_0 M_0 \qquad (A2)$$

in which B_1/i_1 is the field produced per unit current in the detection coil, V is the sample volume, ω_0 is the Larmor frequency, and M_0 is the sample magnetization, given by

$$M_0 = \frac{N_s \gamma^2 \hbar^2 B_p}{4 k_B T}. \tag{A3}$$

Here N_s is the number of protons per unit volume of sample, γ is the gyromagnetic ratio of the proton, and B_p is the polarization field.

Under ideal conditions, the SNR is given simply by the ratio of equation A2 to equation A1. For a sample of fixed dimensions and coil wound from copper wire, the optimal SNR is set by the total mass of conductor used in the receive coil. This is made clear by comparing a coil made with a single layer of wire to a two-layer coil wound with wire of one-half the diameter. The two-layer coil will have four times the B_1/i_1 (twice as many turns per layer and two layers), and so the received signal is a factor of four greater. On the other hand, the resistance per unit length of wire is a factor of four greater, and the total length of wire needed to wind the two layers is a factor of four greater. The result is that the noise in the two layer coil is also increased by a factor of four, and the SNR is unchanged.

While winding a single-layer coil is much easier than a multi-layer coil, there are several compelling reasons for using more layers. First, the larger voltages for both signal and noise from the multi-layer coil enable the coil thermal noise to completely dominate the receiver amplifier noise. Second, when placed in an LC parallel resonant circuit, the higher resistance of the multi-layer coil helps to bring the resonance width up into a useful range, and finally it reduces the tuning capacitance needed. A practical upper limit to the number of turns used is set by the self-resonance frequency of the coil.

Important deviations from the ideal behaviour come from two sources. The first is from pick-up of environmental noise, which in an "urban" environment will often overwhelm the Johnson noise of equation A1 by several orders of magnitude. The second is due to changes in the coil performance due to coupling of the receive coil with other inductive circuits or conductors, such as the polarization coil or shielding, nearby.

The shielding of the receive coil from environmental electromagnetic noise is in principal straightforward. Placing the coil within a conducting enclosure will exclude the environmental noise. The construction of the shield however demands a number of design trade-offs. An effective shield must be several skin-depths thick at the relevant frequencies. The skin-depth of aluminum is approximately 2 mm at 2 kHz. A shield attenuating pick-up by 95% would need to be three skin-depths, or 6 mm thick. The skin depth of copper at the same frequency is 1.5 mm, making a copper shield of similar effectiveness somewhat thinner, but because of copper's much higher density and cost, it would be much heav-

ier and much more expensive. A much thinner shield could be constructed from mild steel, but the magnetic properties would unacceptably perturb the earth's magnetic field. To minimize the size and weight of the shield, one would naturally make it as close as possible in size to the receive coil. Unfortunately, such a shield impacts the performance of the spectrometer as will be described below.

Here, the coupling of the detection coil with the polarization coil increases the effective resistance of the detection coil. In the coil configuration used, the response of the circuit, as measured by the frequency-dependent voltage induced by the field from a small test coil, indicates an effective resistance of 800 Ω. The Q, or quality factor of the circuit measured this way is 5.8.

Inserting the filter bandwidth of 212 Hz, Equation A1 suggests a root-mean-square (rms) noise of 53 nV. This noise is amplified by the circuit Q of 5.8 and the receiver gain of 50000, and then digitized by a 10 bit digitizer with a 5 V full scale. We report signal and noise measurements from the instrument in terms of least significant bits (LSB) of the analog to digital converter, as those most directly reflect the data acquired from it. Each LSB corresponds to 5 V/1024 $\sim$ 4.88 mV. The calculation above yields an expected thermal noise corresponding to 3.2 LSB.

Quantization and nonlinearity imperfections of the analog-to-digital converter are estimated to contribute another 1.25 LSB, added in quadrature with the thermal noise, resulting in an expected rms noise of 3.4 LSB. Noise collected with the coil resonant circuit yields an rms of 7.5 LSB. Much of the 2.2-fold excess noise is concentrated in a small number of harmonics of the power-line frequency, eroding the signal-to-noise ratio in the time domain. These harmonics however do not significantly affect observation of the signal in the frequency domain. Digitally removing the three largest power-line harmonics brings the time-domain noise down to 5.2 LSB, approximately 53% larger than the expected ideal. Given the indoor urban environment and modest shielding used, this is relatively good agreement.

Noise from the receiver and T/R switch relays is negligible, as is demonstrated by the reduction of the noise to an rms of 1.4 LSB when the resonant detection circuit is replaced with a 2 kΩ resistor. In this case, the noise is dominated by the quantization noise of the ADC. The reduction from 7.5 LSB to 1.4 LSB indicates a receiver noise figure of < 0.08 dB; a noiseless amplifier would increase the SNR by no more than 2%.

An approximate numerical calculation for B_1/i_1 gives a value of 23 mT/A, in reasonable agreement with the 24.7 mT/A given in [1]. However, the coupling between the detection coil and polarization coil further perturbs the coil performance, and a direct measurement of B_1/i_1 found from the measured current, 0.833 mA (peak to peak) and nutation frequency (130 Hz) indicates $B_1/i_1 =$ 14.7 mT/A. Taking a sample volume of 0.55 ℓ, $B_p = 10.5$ mT, and discounting the polarization by 0.86 to account

for losses in the adiabatic polarization field turn-off, as described earlier, we expect a signal amplitude of 3.06 μV, or 182 LSB in one transient. The maximum signal observed following a single pulse, 179 LSB, is in excellent agreement with the calculation.

To summarize the effects of the coupling between the detection and polarization coils: the noise is increased, as indicated by the fact that the detection coil effective resistance, 800 Ω is greater than the DC resistance (310 Ω), and the received signal is decreased due to the reduction in B_1/i_1. The net effect of these two factors is a reduction in SNR by a factor of 2.5 compared to that expected from an uncoupled coil. In return however, the shielding provided by the polarization coil provides orders of magnitude reduction in pick up of environmental noise. This factor of 2.5 was expected, as it is identical to the factor described in reference [10], and the detection coil design here follows the design there closely.

Beyond the factor of 2.5, the time-domain SNR here is reduced by a factor of 2.2 due to the pick-up of environmental noise. As described above, most of this noise is concentrated in a small number of power-line harmonics. When the three most significant of these harmonics are removed, the time-domain SNR reduction due to environmental noise becomes a factor of 1.53. In comparison, Callaghan reports the same factor of 2.5 due to coil coupling, and an additional factor of 1.36 due to environmental noise pick-up, but those measurements were made in one of the most electromagnetically quiet environments on the planet, Antarctica, while the measurements here were made in a busy research building located in a major city. Callaghan's SNR calculation predicts an SNR a factor of ~ 3 greater than that here due to the 3-fold greater polarization field used.

[1] Callaghan PT, Eccles CD, Haskell TG, Langhorne PG, and Seymour JD. Earth's field NMR in Antarctica: A pulsed gradient spin echo NMR study of restricted diffusion in sea ice, *J. Magn. Reson.*, **133** 148–54, 1998.

[2] Callaghan PT, Dykstra R, Eccles CD, Haskell TG, and Seymour JD. A nuclear magnetic resonance study of Antarctic sea ice brine diffusivity, *Cold Regions Sci. and Tech.*, **29** 153–71, 1999.

[3] Hunter MW, Dykstra R, Lim MH, Haskell TG, and Callaghan PT. Using earth's field NMR to study brine content in antarctic sea ice: comparison with salinity and temperature estimates, *Appl. Magn. Reson.*, **36** 1–8, 2009.

[4] Duval E, Ranft J, and Bene GJ. Determination des signes relatifs des constantes de couplage 31P-1H dans le tripropyl phosphate par RMN dans le champ magnetique terrestre, *Mol. Phys.*, **9** 427–31, 1965.

[5] Trabesinger AH, McDermott R, Lee SK, Mück M, Clarke J, and Pines A. SQUID-detected liquid state NMR in microtesla fields, *J. Phys. Chem. A*, **108** 957–63, 2004.

[6] Appelt S, Hasing FW, Kuhn H, Sieling U, and Blumich S. Analysis of molecular structures by homo- and heteronuclear J-coupled NMR in ultra-low field, *Chem. Phys. Lett.*, **440** 308–12, 2007.

[7] Appelt S, Glöggler S, Häsing FW, Sieling U, Nejad AG, and Blümich B. NMR spectroscopy in the milli-Tesla regime: Measurement of H-1 chemical-shift differences below the line width, *Chem. Phys. Lett*, **485** 217–20, 2010.

[8] Clarke J, Hatridge M, and Mößle M. SQUID-detected magnetic resonance imaging in microtesla fields, *Annu. Rev. Biomed. Eng.*, **9** 389–413, 2007.

[9] Mohorič A and Stepišnik S. NMR in the Earth's magnetic field, *Prog. Nucl. Magn. Reson. Spect.*, **54** 166–82, 2009.

[10] Callaghan PT, Eccles CD, and Seymour JD. An earth's field nuclear magnetic resonance apparatus suitable for pulsed gradient spin echo measurements of self-diffusion under Antarctic conditions, *Rev. Sci. Instrum.*, **68** 4263–70, 1997.

[11] See http://arduino.cc.

[12] Meiboom S, Gill D. Modified spin-echo method for measuring nuclear relaxation times *Rev. Sci. Instrum.*, **29** 688–91, 1958.

[13] van Duynhoven J, Voda A, Mitek M, Van As H. Time-domain NMR applied to food products, *Ann. Reports on NMR Spectr.* **69** 145–197, 2010.